In: International Journal of Computer Research ISSN: 1535-6698
Volume 17, Issue 4, pp. 1–33

ADVANCED ARRAY PROCESSING TECHNIQUES AND SYSTEMS

Minghui Li*
Department of Electronic & Electrical Engineering, University of Strathclyde
204 George Street, Glasgow G1 1XW, United Kingdom

Abstract

Research and development on smart antennas, which are recognized as a promising technique to improve the performance of mobile communications, have been extensive in the recent years. Smart antennas combine multiple antenna elements with a signal processing capability in both space and time to optimize its radiation and reception pattern automatically in response to the signal environment. This paper concentrates on the signal processing aspects of smart antenna systems. Smart antennas are often classified as either switched-beam or adaptive-array systems, for which a variety of algorithms have been developed to enhance the signal of interest and reject the interference. The antenna systems need to differentiate the desired signal from the interference, and normally requires either *a priori* knowledge or the signal direction to achieve its goal. There exists a variety of methods for direction of arrival (DOA) estimation with conflicting demands of accuracy and computation. Similarly, there are many algorithms to compute array weights to direct the maximum radiation of the array pattern toward the signal and place nulls toward the interference, each with its convergence property and computational complexity. This paper discusses some of the typical algorithms for DOA estimation and beamforming. The concept and details of each algorithm are provided. Smart antennas can significantly help in improving the performance of communication systems by increasing channel capacity and spectrum efficiency, extending range coverage, multiplexing channels with spatial division multiple access (SDMA), and compensating electronically for aperture distortion. They also reduce delay spread, multipath fading, co-channel interference, system complexity, bit error rates, and outage probability. In addition, smart antennas can locate mobile units or assist the location determination through DOA and range estimation. This capability can support and benefit many location-based services including emergency assistance, tracking services, safety services, billing services, and information services such as navigation, weather, traffic, and directory assistance.

Keywords: Array signal processing, Beamforming, Direction-of-Arrival estimation, Smart antennas.

* Corresponding author: Department of Electronic & Electrical Engineering, University of Strathclyde, 204 George Street, Glasgow G1 1XW, United Kingdom, E-mail: Minghui.Li@ieee.org

1. Introduction

The demand for improved performance and increased capacity in mobile communications motivated recent research toward wireless systems that exploit space selectivity and diversity [1]. As a result, there are many efforts on the design of smart antenna arrays. This technology has significant impact on future intelligent transportation systems (ITS). Besides enhancing user capacity, data rates and channel reliability of ITS communications, smart antennas have the capability of locating a vehicle or assisting the location determination through positioning the on-board communication device or a mobile phone [2]. This can support and benefit various transportation applications including automotive telematics and public transit systems, and trigger many location-based services.

Smart antennas have emerged as a promising technique for mobile communication systems to overcome the problem of limited channel bandwidth and satisfy a growing demand for a larger number of mobile terminals on communication channels. The benefits of using smart antennas are that the sender can focus the transmission energy towards the desired user and in a narrower region while minimizing the effect of interference, and the receiver can form a directed beam towards the sender while simultaneously placing nulls in the directions of other transmitters. Furthermore, smart antennas can provide virtual channels in an angle domain by using spatially selective transmission and reception. This is referred to as spatial division multiple access (SDMA), which means that it is possible to multiplex channels in the spatial dimension just as in the frequency and time dimensions. All these help to reduce multipath reflections, delay spread, and co-channel interference, leading to increased network capacity, reduced energy consumption, lower bit error rates (BER), larger range coverage, lower outage probability, and decreased system complexity and infrastructure cost [3].

A myriad of transportation applications can be supported by centralized location and navigation systems, which utilize mobile communication networks and on-board vehicle radio equipment or phones to locate and navigate [4]. Smart antenna arrays can locate mobile units using such estimation models as direction of arrival (DOA), time of arrival (TOA), time difference of arrival (TDOA), and received signal strength (RSS). Various DOA-alone and hybrid positioning systems have been developed in the context of wireless networks. Compared with global positioning system (GPS) based solutions, the network-based schemes save an extra location device, overcome the GPS weakness encountered in urban canyons and indoor environments, and reduce the system complexity, cost and energy consumption. This technology can trigger different location-based services concerning vehicle safety, emergency assistance, vehicle tracking and fleet management, traffic information and directory assistance, and remote vehicle monitoring and services. Moreover, it can aid in the development of vehicle crash avoidance and antitheft systems, and improve the intelligent traffic management and control systems potentially reducing traffic congestion and air pollution [5].

This paper concentrates on the signal processing aspects of smart antenna systems. Any smart antenna design is a trade-off between complexity and performance. Smart

antennas are often classified as either switched-beam systems or adaptive-array systems. The relative merits of both classes of smart antennas, and their application and benefits for ITS are discussed in Section 2. Section 3 describes the array data model pivoting on the narrowband assumption, which is a fundamental concept in wireless DOA estimation and beamforming that allows a small time delay seen by a signal as it propagates across an array to be modeled as a simple phase shift. Once an architecture is chosen for a smart antenna system, an algorithm must be utilized to exploit it. For both switched-beam and adaptive-array systems, a variety of algorithms have been developed to enhance the desired signal while rejecting the interference. Section 4 discusses different beamforming algorithms that exploit the spatial and/or temporal characteristics of a reference signal. There exists a myriad of methods for DOA estimation with conflicting demands of accuracy and computation cost. Section 5 discusses some of the high resolution algorithms, their performance is analyzed and compared, and the pros and cons of each algorithm are discussed.

2. Smart Antennas and Their Benefits to Communication Systems

ITS communications can benefit from antenna array technology through exploiting either spatial selectivity or spatial diversity. Spatial selectivity separates spectrally and temporally overlapping signals through beamforming while minimizing interference, and diversity processing takes advantages of the different fading observed by antennas that are widely separated. In the literature, the term of “smart antennas” is often used to describe beamforming based technology and systems, on which we put the focus of this chapter.

2.a. Types of Smart Antennas

Smart antennas are usually categorized as either switched-beam or adaptive-array systems according to how they produce their response [6]-[7].

A *switched-beam system* is a system that can choose from many predefined patterns, in order to enhance the received signal. It is considered as an extension of the cell-sectoring scheme, in which a cell is composed of three 120-degree macro-sectors. The switched-beam method further subdivides the macro-sectors into several micro-sectors. Each micro-sector contains a predetermined fixed beam pattern. As a mobile user moves throughout the cell, the switched-beam system detects the signal strength, chooses the micro-sector containing the strongest signal, and continually switches the beams as necessary. Switched-beam systems provide range extension and enhanced coverage. Compared to conventional sectored cells, switched-beam systems may increase the range of a base station from 20% to 200% [3]. Less complexity in signal processing leads to its cost efficiency. At the same time, this technique has some apparent disadvantages. Since the beams are predefined and fixed, the signal strength varies as the user moves through

the micro-sector. In addition, a switched-beam system does not discriminate between the desired signal and interference. If an interferer is near the center of the selected beam, it may be enhanced more than the desired user.

Adaptive-array systems take a very different approach and have the ability to adapt the radiation pattern to the signal environment in real time. The adaptive-array system continuously distinguishes among desired signals, multipath, and interfering signals according to their spatial and/or temporal characteristics, and updates its beam pattern based on changes in both the desired and interfering signal parameters. Adaptive-array systems can customize an appropriate radiation pattern for each individual user, which is far superior to the performance of a switched-beam system. Adaptive-array systems locate and smoothly track the desired user with main lobe and interferers with nulls, and dynamically adjust the beam pattern to enhance reception while minimizing interference.

Figure 1 illustrates the beam patterns that might be chosen by a switch-beam system and an adaptive-array system, in a scenario involving a desired user and an interferer. Both systems direct their main lobe in the general direction of the desired user, but the adaptive-array system makes a more accurate placement. On the contrary, the switched-beam system is not only unable to place the desired signal at the maximum of the main lobe, but also unable to fully reject the interference.

Although providing lower gain and limited interference suppression, switched-beam systems are simple and can be easily deployed. This makes it attractive in some ITS applications, for example ITS sensor networks. Wireless sensor network (WSN) is a flexible and scalable paradigm that is drawing increasing attention from ITS community [8]-[10]. A key point to increase the reliability of a WSN is to improve the efficiency of wireless links. Adaptive arrays are generally too complex due to the size and cost constraints typical of sensor nodes, but the simpler switch-beam counterpart seems feasible. A system consisting of four fixed beam antennas is presented in [11], in which the beam selection is implemented through two digital lines based on the received signal strength. The simple system demonstrates substantial benefits: it extends the communication range by more than 250% when used outdoors, and it suppresses multipath fading by more than 70% while indoors.

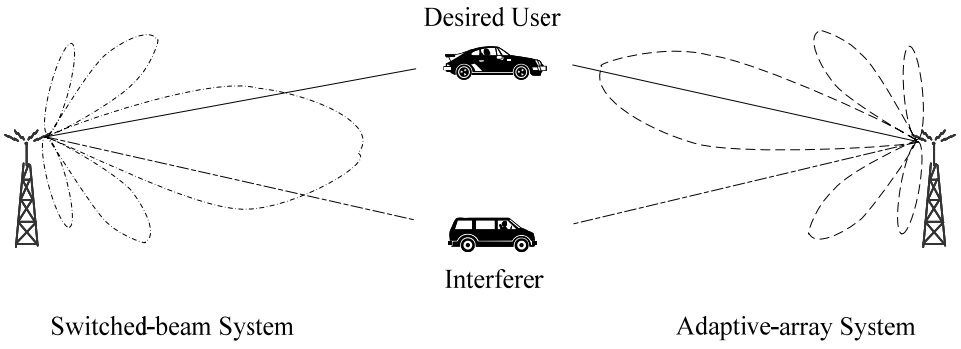

Figure 1. Beamforming lobes and nulls that switched-beam and adaptive-array systems might have for identical user-interferer scenarios.

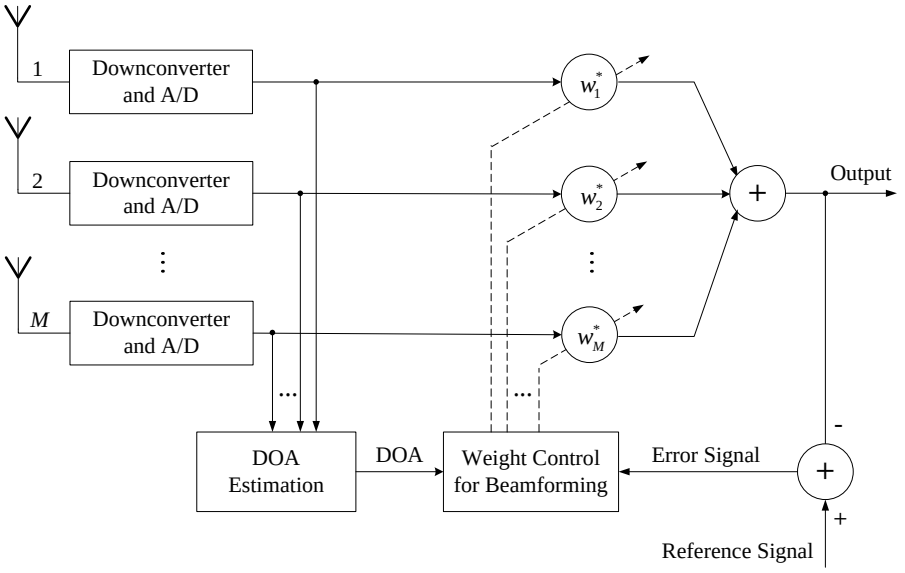

Figure 2. Functional block diagram of adaptive array systems.

Adaptive-array systems, considered by many to be "smarter" than switched-beam systems, are growing in popularity in mobile communications. A functional block diagram of adaptive arrays is shown in Figure 2. Rather than choosing a beam from predefined patterns, adaptive-array systems synthesize patterns by dynamically changing the weights (amplitudes and phases of the signals). The central part of an adaptive array is the beamformer, which applies a complex weight to each signal and sums the weighted signals. The weights are computed using the direction of the desired signal (spatial reference) or a training sequence (temporal reference). Section 4 deals with some of the beamforming algorithms. DOA estimators measure the signal directions by computing the time delays among the antenna elements, which are discussed in Section 5.

Adaptive-array systems are most effective when the communication standard is designed to accommodate the adaptive array technology. As a result, medium access control (MAC) protocols that support adaptive-array and switched-beam systems in wireless networks have been developed [12]-[14].

2.b. Benefits of Smart Antennas for ITS

Smart antennas, when used appropriately, help to enhance ITS communications by increasing channel capacity and spectrum efficiency, extending range coverage, multiplexing channels with space division multiple access (SDMA), and compensating electronically for aperture distortion. Moreover, smart antennas can locate on-board vehicle mobile units, and thus enable numerous location-based service and applications.

2.b.1. Spatial filtering for interference reduction

As shown in Figure 1, smart antennas attempt to enhance the received signal and reject all interfering signals through spatial filtering, and improve the signal to interference and noise ratio (SINR). This can reduce delay spread, multipath fading, co-channel interference, bit error rate, system complexity, and outage probability.

In noise or interference limited environments, the antenna array gain can be exchanged for higher detection probability and lower BER. The probability of detection in the case where a matched filter is employed for each array element is given by [15]

$$P_D = Q\left(Q^{-1}\left(P_F\right) - \sqrt{M \cdot SNR}\right), \tag{1}$$

where $Q(\bullet)$ is the *Q* function defined by $Q(\alpha) = \frac{1}{\sqrt{2\pi}} \int_{\alpha}^{\infty} e^{-\frac{x^2}{2}} dx$, P_F is the threshold false alarm probability, and *M* is the number of elements. The approximate formula for the BER in a CDMA system is given by [16]

$$P_b = Q\left(\sqrt{3 \cdot SF \cdot SIR_{omni} \cdot k^{-1}}\right), \tag{2}$$

where *SF* is the spreading factor, SIR_{omni} is the signal to interference ratio with an omnidirectional antenna, and

$$k = \frac{BW}{360} + SLL\left(1 - \frac{BW}{360}\right), \tag{3}$$

with BW and SLL the effective beamwidth and average sidelobe level, respectively. Smart antennas can increase the network coverage through antenna directivity and interference reduction. With small angular spread and the Hata path loss model, the range extension factor, *REF*, can be calculated as [17]

$$REF = \frac{r_2}{r_1} = M^{0.3}, \tag{4}$$

where r_1 and r_2 are the ranges with a single antenna and array, respectively. The range extension with smart antennas can lead to reduction in the number of base stations needed to serve the same area, and consequently reduce the infrastructure costs. The base station array gain can also be exploited to reduce the power transmitted by the mobile, which may relax the battery requirements, reduce the handset size and weight, and mitigate interference to other users. Smart antennas can increase the capacity through SNR improvement and co-channel interference rejection, as shown by the Shannon's expression for the capacity of a channel with bandwidth *W* and with additive Gaussian noise [16]

$$C = W \log_2\left(1 + SNR\right) \quad \left(bit/s\right). \tag{5}$$

Smart antennas can also exploit spatial diversity [18], multiple-input multiple-output (MIMO) technology [19], and SDMA to enhance the user capacity.

2.b.2. Space division multiple access (SDMA)

Smart antennas can be used to implement SDMA, which is among the most sophisticated utilization of smart antenna technology. It uses independently steered beams at the same frequency to support multiple users within a cell, as shown in Figure 3. This means that multiple users within the same cell can operate on the same time and frequency channel by exploiting the spatial separation of the users. With SDMA, it is possible to multiplex channels in the spatial dimension just as in the frequency and time dimensions, and this can be exploited as a hybrid multiple access technique complementing TDMA, FDMA and CDMA [20]. This concept can be seen as a dynamic (as opposed to fixed) sectoring approach in which each user defines its own sector as it moves. Through providing virtual channels in an angle domain, SDMA dramatically increases frequency reuse while it greatly improves the interference suppression capability, resulting in increased capacity and reduced infrastructure cost. SDMA enables capacity increases not only through inter-cell frequency reuse, but also through intra-cell frequency reuse [1].

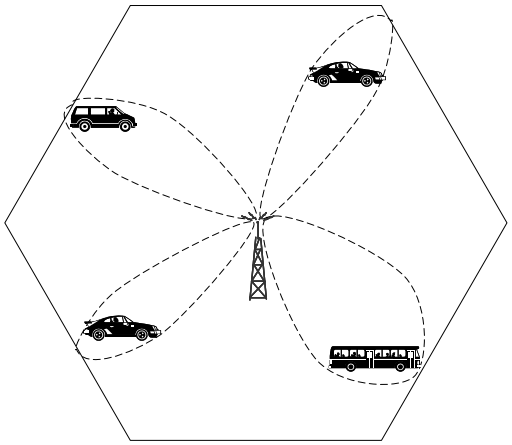

Figure 3. Base station employing SDMA. Four independent beams at the same frequency support four users within the same cell.

2.b.3. Location positioning of mobile units

Vehicle location and navigation using communication networks and the on-board mobile units have received considerable attention around the world, which will benefit many applications such as automotive telematics and modern public transit systems [4]. This technology will have significant impact on future intelligent transportation systems. Besides emergency assistance, mobile unit localization can trigger many location-based services for intelligent transportation applications, which can be categorized into safety, information, tracking, remote, and billing services. Safety services, especially personal safety, are often the top priority in ITS. Information services include weather, traffic, navigation, and directory assistance. Tracking services can monitor continuously the

location of the vehicle, asset, and people, which facilitate vehicle and fleet management. Remote services can provide further convenience as unlocking the car, monitoring the engine, and collecting tolls. Location-sensitive billing will be able to differentiate a variety of customer services. Furthermore, the location service can aid in the development of vehicle crash avoidance and antitheft systems, and improve the intelligent traffic management and control systems potentially reducing traffic congestion and air pollution. In addition, location of mobile users can be exploited to increase communications capacity through dynamic reuse planning. With user location information, channels can be assigned dynamically to areas of high user density and hence better capacity can be achieved [3].

Smart antennas can determine the mobile unit location or assist the location determination based on the wireless network infrastructure using estimation models, such as DOA, TOA and TDOA [21]-[24]. Those network-based location schemes are of considerable interest in ITS, and often outperform the schemes depending on GPS, because the network-based methods save an extra location device, overcome the GPS weakness encountered in urban canyons and indoor environments, and reduce the system complexity, cost and energy consumption [4]. DOA and range estimation is a basic capability of an antenna array, and a myriad of high resolution algorithms have been proposed. Various DOA-alone [25]-[27] and hybrid positioning systems [28]-[30] using communications infrastructure have been developed, including hybrid DOA-TOA systems, DOA-TDOA systems, and etc. It is demonstrated that the combination of disparate data through data fusion produces more accurate location estimates than any of the individual measurement [31].

3. Array Data Model and Problem Formulation

To understand how multiple antennas can be exploited for beamforming and DOA estimation, we must first model the signals received at the array. Consider a general scenario of an array of *M* elements arranged in an arbitrary geometry immersed in the far field (planar wave) of *N* point sources at unknown locations. To simplify the exposition, our discussion is confined to azimuth-only systems, i.e., the sensors and signals are assumed to be co-planar. However, the data model and algorithms presented here are general and the extension to azimuth-and-elevation systems is straightforward.

We start our discussion by considering the situation of a single source. Let $x(t)$ denote the signal as measured at a reference point, for instance the first sensor. The output of sensor k ($k = 1,\ldots,M$) can be written as

$$\bar{y}_k(t) = \bar{h}_k(t) * x(t - \tau_k) + \bar{n}_k(t), \tag{6}$$

where $\bar{h}_k(t)$ is the impulse response of the kth sensor, $*$ denotes the convolution operation, τ_k denotes the time needed for the wave to travel from the reference point to sensor k, and $\bar{n}_k(t)$ is an additive noise. The array is assumed to be calibrated, i.e., the

sensors are modeled as linear time invariant systems with known $\bar{h}_k(t)$ and known locations. The Fourier transform of the model (6) is given by

$$\bar{Y}_k(\omega) = \bar{H}_k(\omega) X(\omega) e^{-j\omega\tau_k} + \bar{N}_k(\omega), \tag{7}$$

where $\bar{Y}_k(\omega)$, $\bar{H}_k(\omega)$, $X(\omega)$ and $\bar{N}_k(\omega)$ denote the Fourier transforms of $\bar{y}_k(t)$, $\bar{h}_k(t)$, $x(t)$ and $\bar{n}_k(t)$, respectively, which are defined as, e.g., $X(\omega) = \int_{-\infty}^{\infty} x(t) e^{-j\omega t} dt$.

For a general class of physical signals, such as the carrier modulated signals encountered in communications, the signal is bandpass and its spectrum is limited to a certain band of frequencies centered about the carrier frequency ω_c. Assume that $x(t)$ is a bandpass signal, and $s(t)$ denotes the baseband signal associated with $x(t)$, which is often termed the complex envelope. $x(t)$ is assumed to be obtained by real modulation process, that is

$$x(t) = s(t) e^{j\omega_c t} + \left[s(t) e^{j\omega_c t} \right]^* = 2\,\mathrm{Re}\left[s(t) e^{j\omega_c t} \right], \tag{8}$$

where $(\bullet)^*$ denotes complex conjugate, and $\mathrm{Re}[\bullet]$ represents the real part. In the frequency domain,

$$X(\omega) = S(\omega - \omega_c) + S^*\left(-(\omega + \omega_c)\right), \tag{9}$$

where $S(\omega) = \int_{-\infty}^{\infty} s(t) e^{-j\omega t} dt$. When insert $X(\omega)$ (9) into (7), we obtain

$$\bar{Y}_k(\omega) = \bar{H}_k(\omega)\left[S(\omega - \omega_c) + S^*\left(-(\omega + \omega_c)\right)\right] e^{-j\omega\tau_k} + \bar{N}_k(\omega). \tag{10}$$

Consider a classic receiver model depicted in Figure 4: to obtain the baseband signal $y_k(t)$, the received signal $\bar{y}_k(t)$ is demodulated and filtered with a baseband (lowpass) filter. Let $\tilde{y}_k(t)$ denote the demodulated signal $\tilde{y}_k(t) = \bar{y}_k(t) e^{-j\omega_c t}$, whose Fourier transform is given by

$$\tilde{Y}_k(\omega) = \bar{H}_k(\omega + \omega_c)\left[S(\omega) + S^*\left(-(\omega + 2\omega_c)\right)\right] e^{-j(\omega+\omega_c)\tau_k} + \bar{N}_k(\omega + \omega_c). \tag{11}$$

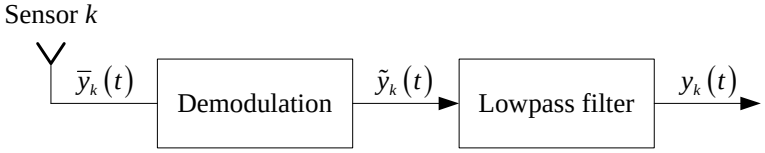

Figure 4. Simplified block diagram of the analog processing in a receiver system.

When $\tilde{y}_k(t)$ is passed through a lowpass filter with bandwidth matched to $S(\omega)$, the components centered at $\omega = -2\omega_c$ is eliminated. Hence, the output signal can be expressed as

$$Y_k(\omega) = H_k(\omega+\omega_c)S(\omega)e^{-j(\omega+\omega_c)\tau_k} + N_k(\omega+\omega_c), \tag{12}$$

where $H_k(\omega+\omega_c)$ and $N_k(\omega+\omega_c)$ denote the parts of $\bar{H}_k(\omega+\omega_c)$ and $\bar{N}_k(\omega+\omega_c)$ that fall within the passband of the lowpass filter.

Now, we make the narrowband assumption: the received signals are narrowband, so that $|S(\omega)|$ decreases rapidly with increasing $|\omega|$. (12) can be reduced to the following equation in an approximate way,

$$Y_k(\omega) = H_k(\omega_c)S(\omega)e^{-j\omega_c\tau_k} + N_k(\omega+\omega_c), \tag{13}$$

whose time-domain counterpart is the following

$$y_k(t) = H_k(\omega_c)e^{-j\omega_c\tau_k}s(t) + n_k(t), \tag{14}$$

where the baseband signals $y_k(t)$ and $n_k(t)$ are the inverse Fourier transforms of $Y_k(\omega)$ and $N_k(\omega+\omega_c)$, respectively. Under the narrowband assumption, the array model (6) is simplified in that the time delay τ_k is modeled as a simple phase shift, and the sensor frequency response is flat over the signal bandwidth (but may vary with the source direction).

We introduce the so-called array steering vector

$$\mathbf{a}(\theta) = \left[H_1(\omega_c)e^{-j\omega_c\tau_1} \ldots H_M(\omega_c)e^{-j\omega_c\tau_M}\right]^T, \tag{15}$$

where θ is the source DOA, and $[\bullet]^T$ denotes the transpose. By making use of (15), the array model can be expressed as

$$\mathbf{y}(t) = \mathbf{a}(\theta)s(t) + \mathbf{n}(t), \tag{16}$$

where

$$\mathbf{y}(t) = \left[y_1(t) \ldots y_M(t)\right]^T,$$

$$\mathbf{n}(t) = \left[n_1(t) \ldots n_M(t)\right]^T,$$

denote the array output vector and additive noise vector, respectively. In most mobile communication applications, the first sensor is selected as the reference point, and the

sensors are assumed to be omnidirectional over the DOA range of interest with unit gain, the expression (15) can be simplified to the following form

$$\mathbf{a}(\theta) = \begin{bmatrix} 1 & e^{-j\omega_c \tau_2} \ldots e^{-j\omega_c \tau_M} \end{bmatrix}^T . \tag{17}$$

The extension of (16) to multiple sources is straightforward. Based on the assumption of linear sensors and superposition principle, the array data model for *N* sources is given by

$$\mathbf{y}(t) = \mathbf{A}(\boldsymbol{\theta})\mathbf{s}(t) + \mathbf{n}(t), \tag{18}$$

where

$$\mathbf{A}(\boldsymbol{\theta}) = \left[\mathbf{a}(\theta_1) \ldots \mathbf{a}(\theta_N) \right],$$

$$\mathbf{s}(t) = \left[s_1(t) \ldots s_N(t) \right]^T,$$

denote the array transfer matrix and source signal vector, respectively.

The dependence of τ_k in (17) as a function of source direction θ can be derived using the planar wave assumption. As an example, we consider a uniform linear array (ULA) of *M* sensors with inter-element spacing *d* and a signal illuminating the array from θ as depicted in Figure 5. The first element is chosen as the reference point, we find that

$$\tau_k = \frac{(k-1)d\sin\theta}{c}, \quad k = 1, \ldots, M \tag{19}$$

where *c* is the propagation velocity of the incident wave.

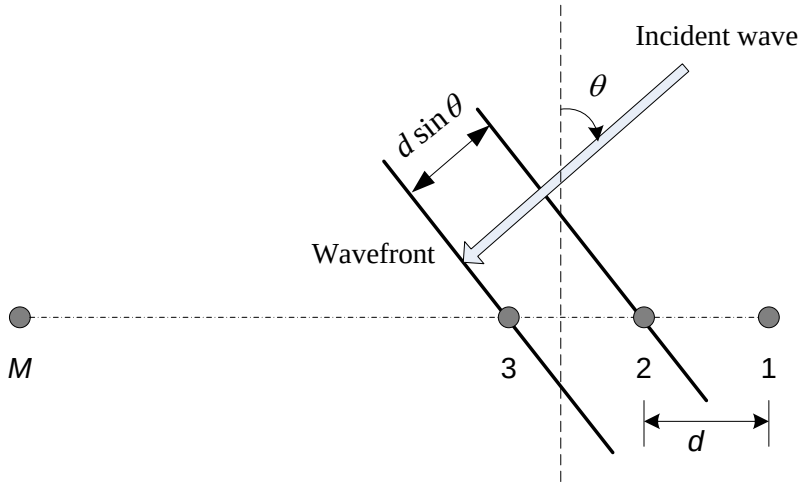

Figure. 5 Uniform linear array scenario.

An array can be considered to sample the wavefield spatially, and the sensor outputs can be viewed as a group of discrete time samples of the incident signal with sampling interval $\tau = d\sin\theta / c$, and sampling frequency is given by

$$f_s = \frac{1}{\tau} = \frac{c}{d\sin\theta}. \tag{20}$$

The minimum sampling rate occurs when $\sin\theta = 1$

$$f_{s\min} = \frac{c}{d}. \tag{21}$$

From the Nyquist sampling theorem for a narrowband signal at ω_c, $f_s \geq 2f_c$, therefore, we have

$$d \leq \frac{\lambda}{2}, \tag{22}$$

where λ is the signal wavelength. The equation (22) can be interpreted as a spatial Nyquist sampling theorem, which states that the inter-element space should be smaller than half of the signal wavelength to avoid spatial aliasing.

The steering vector $\mathbf{a}(\theta)$ describes a mapping between DOA and array response, and provides a framework for describing more complex phenomena including multipath, fading, and angle spread. In theory, $\mathbf{a}(\theta)$ is completely defined by the array geometry and the gain patterns of individual antenna elements, as in (15). However, in practice, the actual array response can deviate significantly from its analytic form, due to the effect of mutual coupling, uncertainty in antenna locations, gain and phase errors, and etc. The process of determining $\mathbf{a}(\theta)$ as a function of θ is known as array calibration, which is accomplished by placing a transmitter at a known angle and estimating $\mathbf{a}(\theta)$ from the received data [32].

The vectors of signals and noise are assumed to be stationary, temporally white, zero-mean complex Gaussian random processes with second-order moments given by

$$\begin{aligned} E\left\{\mathbf{s}(t)\mathbf{s}^H(s)\right\} &= \mathbf{P}\delta_{ts} \\ E\left\{\mathbf{s}(t)\mathbf{s}^T(s)\right\} &= 0 \\ E\left\{\mathbf{n}(t)\mathbf{n}^H(s)\right\} &= \sigma_n^2\mathbf{I}\delta_{ts} \\ E\left\{\mathbf{n}(t)\mathbf{n}^T(s)\right\} &= 0 \end{aligned} \tag{23}$$

where δ_{ts} is the Kronecker delta, $(\bullet)^H$ denotes complex conjugate transpose, $E\{\bullet\}$ stands for expectation, and $\mathbf{P}$ and $\sigma_n^2\mathbf{I}$ are the signal and noise covariance matrices, respectively.

Assuming that the noise and signals are independent, the data covariance matrix is given by

$$\mathbf{R} = E\left\{\mathbf{y}(t)\mathbf{y}^H(t)\right\} = \mathbf{A}\mathbf{P}\mathbf{A}^H + \sigma_n^2\mathbf{I}. \tag{24}$$

An unbiased estimate of $\mathbf{R}$ using L data samples can be obtained using an averaging scheme

$$\hat{\mathbf{R}} = \frac{1}{L}\sum_{t=1}^{L}\mathbf{y}(t)\mathbf{y}^H(t). \tag{25}$$

4. Beamforming Algorithms

A beamformer is a device that applies a complex weight w_i, $i = 1, \cdots, M$ to the signal $y_i(t)$ of each antenna element and sums the weighted signals, as illustrated in Figure 6. The array gain pattern is defined by

$$F(\theta) = \left|\mathbf{w}^H\mathbf{a}(\theta)\right|^2, \tag{26}$$

where $\mathbf{w} = \left[w_1 \ldots w_M\right]^T$. The gain pattern describes the power in the beamformer output due to a signal impinging on the array from a particular direction θ. A judicious choice of the weights will result in a desirable beam pattern such as that of Figure 1. The beamformer usually requires either the source directions (spatial characteristics) or reference signals (temporal characteristics) to compute the weights. In this section, we discuss three techniques using spatial reference, one technique using temporal reference, and the adaptive implementations of these algorithms that adjust the weights in real time to track the signal environment changes. Many wireless standards specify that users should periodically transmit a known signal, often called a training sequence, over a specified interval for channel estimation. These known signals can be exploited as the reference signal. Source bearings can be measured using DOA estimation algorithms.

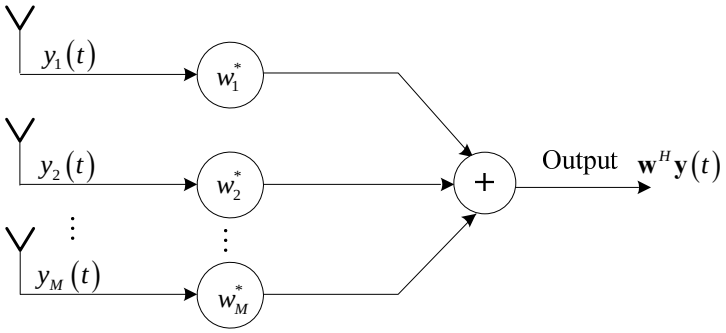

Figure 6. Narrowband beamforming structure.

4.a. Conventional Beamformer

Conventional beamformer, also known as delay-and-sum beamformer, is one of the oldest and simplest array processing algorithms [33]. The underlying idea is quite simple: when a propagating signal is present in an array's aperture, if the sensor outputs are delayed by appropriate amounts and added together, the signal will be reinforced with respect to noise or waves propagating in different directions [34]. For conventional beamformer, all the weights have equal magnitudes, and the phases (time delays) are selected based on the length of time it takes for the signal to propagate between sensors. To steer the array in a particular direction θ_d, the weights are selected as

$$\mathbf{w} = \frac{1}{M}\mathbf{a}(\theta_d). \tag{27}$$

The process is similar to steering the array mechanically in the look direction except that it is done electronically by adjusting the phases. In an environment consisting of only one source of power p_s in the array look direction θ_d and uncorrelated noise, using the data model (18) and (24), the output power of the beamformer can be measured as

$$\begin{aligned} P(\theta_d) &= E\left\{\left|\mathbf{w}^H\mathbf{y}(t)\right|^2\right\} \\ &= \frac{\mathbf{a}^H(\theta_d)\mathbf{R}\,\mathbf{a}(\theta_d)}{M^2} \\ &= \frac{\mathbf{a}^H(\theta_d)\left[\mathbf{a}(\theta_d)p_s\mathbf{a}^H(\theta_d)+\sigma_n^2\mathbf{I}\right]\mathbf{a}(\theta_d)}{M^2} \\ &= p_s + \frac{\sigma_n^2}{M}. \end{aligned} \tag{28}$$

The first part represents the output signal power, which is the same as the source power, and the second part represents the output noise power. Therefore, the array with these weights (27) has unity response in the look direction, and the array gain, which is defined as the ratio of the output SNR to the input SNR, equals to *M*, the number of elements. Though the conventional beamformer provides maximum SNR when there is no directional interference, it is not effective in the presence of directional jammers, intentional or unintentional.

4.b. Null-steering Beamformer

A null-steering beamformer can cancel a plane wave arriving from a known direction by producing a null in the response pattern in that direction. A beam with unity response in the desired direction θ_d and nulls in k interference directions $\theta_1,\cdots,\theta_k$ may be formed by estimating the weights of a beamformer using suitable constraints [35]. The desired weight vector is the solution to following simultaneous equations:

$$\begin{aligned} \mathbf{w}^H \mathbf{a}(\theta_d) &= 1 \\ \mathbf{w}^H \mathbf{a}(\theta_i) &= 0, \quad i = 1, \cdots, k. \end{aligned} \tag{29}$$

Using matrix notation, this becomes

$$\mathbf{w}^H \mathbf{C} = \boldsymbol{\delta}_1^T, \tag{30}$$

where

$$\begin{aligned} \mathbf{C} &= \left[\mathbf{a}(\theta_d) \ \mathbf{a}(\theta_1) \cdots \ \mathbf{a}(\theta_k) \right], \\ \boldsymbol{\delta}_1 &= \left[1 \ 0 \cdots \ 0 \right]^T. \end{aligned}$$

In a general scenario where **C** is not a square matrix, a suitable estimate of the weight vector may be computed using

$$\mathbf{w} = \left(\boldsymbol{\delta}_1^T \mathbf{C}^H \left(\mathbf{C}\mathbf{C}^H \right)^{-1} \right)^H. \tag{31}$$

Although the beam pattern produced by this beamformer has nulls in the directions of interferences, it is not designed to minimize the noise at the array output. A performance analysis of the null-steering algorithm is presented in [36].

Another class of approaches for null-steering beamforming is array pattern synthesis, which is to determine a set of weights that result in a prescribed and somewhat arbitrary beam pattern response. In general, array pattern synthesis is first formulated as an optimization problem with the goal of sidelobe level (SLL) suppression and/or null placement in certain directions, while preserving the gain of the main beam toward the desired direction, and then solved by a global search algorithm such as simulated annealing [37], genetic algorithms [38], and particle swarm optimization algorithms [39] for the optimal weight vector. Compared with the constraint-based method, this approach has some obvious advantages: a) the SLL and the null location, width and depth can be fully controlled; b) wide null placement is possible for nulling interference with angle spread; c) flat sidelobe and nulls can be produced, which facilitates minimizing interference over a large area [38], [40]. All these features make this technique extremely attractive for beam pattern design of a transmitting array.

4.c. Optimal Beamformer

The optimal beamformer, also known as the minimum variance distortionless response (MVDR) beamformer [41], does not require either the knowledge of the directions and power levels of the interferers, or the level of the background noise power, to maximize the output SNR. It only requires the DOA of the desired signal. This beamformer is also known as the maximum likelihood (ML) filter [41],since it finds the ML estimate of the

power of the signal source assuming all sources as interference, and the weights are the solution to the following constrained optimization problem

$$\min_{\mathbf{w}} E\left\{\left|\ \mathbf{w}^H\mathbf{y}(t)\ \right|^2\right\} \quad \text{subject to } \mathbf{w}^H\mathbf{a}(\theta_d)=1. \tag{32}$$

The constraint $\mathbf{w}^H\mathbf{a}(\theta_d)=1$ ensures that the desired signal coming from the DOA θ_d passes to the beamformer's output undistorted. This process is to minimize the mean output power $E\left\{\left|\mathbf{w}^H\mathbf{y}(t)\right|^2\right\}$ while maintaining unity response in the look direction. Solving the optimization problem amounts to finding the set of weights that result in the lowest-power array output subject to the directional constraint, while minimizing power presumably reduces the deleterious effects of noise and unwanted signals. To minimize the total output noise while keeping the output signal constant is the same as maximizing the output SNR.

Using the Lagrange method, we can solve the constraint problem, and the expression for the weights is given by

$$\mathbf{w}=\frac{\mathbf{R}^{-1}\mathbf{a}(\theta_d)}{\mathbf{a}^H(\theta_d)\mathbf{R}^{-1}\mathbf{a}(\theta_d)}, \tag{33}$$

where θ_d is the DOA of the desired signal. This scheme requires the number of interferers to be less than or equal to $M-2$, since an array with *M* elements has $M-1$ degrees of freedom, and one has been utilized by the constraint in the look direction. Multipath arrivals in wireless communication environment may violate this condition, and the beamformer may not be able to achieve the maximization of the output SNR by suppressing all interferers. However, as argued in [42], the beamformer does not have to fully suppress interference, since a few decibels increase in the output SNR can make a large improvement in the channel capacity. The applications of optimal beamformer in mobile communications for interference cancelation and performance improvement are addressed in [42]-[44].

4.d. Minimum Mean Square Error (MMSE) Beamformer

This beamformer requires a reference signal instead of the desired signal direction [45]. As shown in Figure 2, the array output $\mathbf{w}^H\mathbf{y}(t)$ is subtracted from a reference signal $d(t)$ to generate an error signal $e(t)=d(t)-\mathbf{w}^H\mathbf{y}(t)$, which is used to estimate the weights. The beamformer that extracts the desired signal should minimize the error signal in some sense, for example the mean square error (MSE), and this is the motivation for the minimum mean square error (MMSE) beamformer. The MSE is defined as

$$E\left\{\left|e(t)\right|^2\right\} = E\left\{\left|d(t) - \mathbf{w}^H\mathbf{y}(t)\right|^2\right\} = E\left\{\left|d(t)\right|^2\right\} - \mathbf{r}_{yd}^H\mathbf{w} - \mathbf{w}^H\mathbf{r}_{yd} + \mathbf{w}^H\mathbf{R}\mathbf{w}, \tag{34}$$

where $\mathbf{r}_{yd} = E\{\mathbf{y}(t)d^*(t)\}$, and $\mathbf{R} = E\{\mathbf{y}(t)\mathbf{y}^H(t)\}$. Setting the gradient of $E\left\{\left|e(t)\right|^2\right\}$ with respect to $\mathbf{w}^*$ equal to zero yields the well-known Wiener-Hoff solution for the optimal weight vector

$$\mathbf{w} = \mathbf{R}^{-1}\mathbf{r}_{yd}, \tag{35}$$

and the corresponding MMSE of the beamformer is given by

$$MMSE = E\left\{\left|d(t)\right|^2\right\} - \mathbf{r}_{yd}^H\mathbf{R}^{-1}\mathbf{r}_{yd}. \tag{36}$$

In general, the MMSE beamformer provides higher output SNR compared to the MVDR beamformer in the presence of a weak signal source. As the input signal power becomes large compared to the background noise, the two beamformers produce almost the same results [45]. The enhanced SNR by MMSE beamformer is achieved at the cost of signal distortion by the processor, while the MVDR beamformer is distortionless. Use of reference signals for computing array weights in mobile communications is reported in [46]-[47].

4.e. Adaptive Beamforming Algorithms

The methods presented in the previous paragraphs all require knowledge of the channel statistics, for example the data covariance matrix **R**. In conventional and null-steering beamformers, **R** is required for source DOA estimation; in MVDR beamformer, **R** is used for DOA estimation and weights computation; and in MMSE beamformer, **R** and $\mathbf{r}_{yd}$ are needed for weights estimation. In a practical situation when **R** is unknown, adaptive algorithms can be used to adjust the weights in a recursive manner and track changes in the user signals and interference.

4.e.1. Sample Matrix Inversion (SMI) Algorithm

This method computes the array weights by replacing **R** with its estimates. An unbiased estimate of **R** using L samples $\mathbf{y}(n)$, $n = 1,\ldots,L$, is given by $\hat{\mathbf{R}} = \frac{1}{L}\sum_{n=1}^{L}\mathbf{y}(n)\mathbf{y}^H(n)$. When new samples arrive, $\hat{\mathbf{R}}$ can be updated using

$$\hat{\mathbf{R}}(n+1) = \frac{n\hat{\mathbf{R}}(n) + \mathbf{y}(n+1)\mathbf{y}^H(n+1)}{n+1}, \tag{37}$$

and $\hat{\mathbf{R}}^{-1}$ can be obtained using the matrix inversion lemma as follows

$$\hat{\mathbf{R}}^{-1}(n+1) = \hat{\mathbf{R}}^{-1}(n) - \frac{\hat{\mathbf{R}}^{-1}(n)\mathbf{y}(n+1)\mathbf{y}^{H}(n+1)\hat{\mathbf{R}}^{-1}(n)}{1+\mathbf{y}^{H}(n+1)\hat{\mathbf{R}}^{-1}(n)\mathbf{y}(n+1)}, \tag{38}$$

with

$$\hat{\mathbf{R}}^{-1}(1) = \frac{1}{\varepsilon}\mathbf{I}, \quad \varepsilon > 0. \tag{39}$$

A new estimate of the weights $\mathbf{w}_{n+1}$ at time instant $n+1$ can be made using $\hat{\mathbf{R}}(n+1)$ and $\hat{\mathbf{R}}^{-1}(n+1)$. As the number of samples grows, the estimates $\hat{\mathbf{R}}$ and $\hat{\mathbf{R}}^{-1}$ approach their true values $\mathbf{R}$ and $\mathbf{R}^{-1}$, and thus the estimated weights approach the desired weight. Application of SMI for weights estimation in wireless communications has been investigated in [20], [47]-[49].

4.e.2. Least Mean Square (LMS) Algorithm

LMS is one of the most well-known adaptive algorithms [50]. Consider the cost function (34) of MMSE beamformer using a reference signal. This function is an *M* dimensional quadratic function. A simple recursive procedure for determining the minimum of the quadratic is to update the estimate by an amount proportional to the negative gradient of the error, that is

$$\mathbf{w}_{n+1} = \mathbf{w}_n - \mu\nabla_{\mathbf{w}_n^*} E\left\{|e_n|^2\right\}, \tag{40}$$

where *n* is the iteration index, μ is a positive scalar that regulates the step size and controls the convergence characteristic of the algorithm, $e_n = d(n) - \mathbf{w}_n^H\mathbf{y}(n)$, and the gradient is given by

$$\nabla_{\mathbf{w}_n^*} E\left\{|e_n|^2\right\} = 2E\left\{e_n \cdot \nabla_{\mathbf{w}_n^*}\left(e_n^*\right)\right\} = -2E\left\{e_n\mathbf{y}_n^*\right\}. \tag{41}$$

Therefore, the weights update equation can be rewritten as

$$\mathbf{w}_{n+1} = \mathbf{w}_n + \mu E\left\{e_n\mathbf{y}_n^*\right\}. \tag{42}$$

To ease the notion, μ is still used in (42). In its standard form, the LMS algorithm uses an instantaneous, and hence, noisy estimate of the gradient to replace the statistical gradient estimate (41). In general, the LMS algorithm iteratively finds the weight vector that minimizes the MSE cost function $E\left\{|e_n|^2\right\}$ by estimating $E\left\{e_n\mathbf{y}_n^*\right\}$ with $e_n\mathbf{y}_n^*$, a

product of the array signals and the error between the reference signal and the array output, and the weight update equation is given by

$$\mathbf{w}_{n+1} = \mathbf{w}_n + \mu e_n \mathbf{y}_n^*, \tag{43}$$

where $e_n = d_n - \mathbf{w}_n^H \mathbf{y}_n$. The most attractive feature of the LMS algorithm is its low computational complexity, and the main drawback of this technique is its slow convergence rate if μ is too small, and potential for instability if μ is too large. There are ways to adjust μ to make a prudent trade-off between stability and speed of convergence [51]. Its use for mobile communication systems has been studied in [42]-[43], [52].

When both source directions and training sequences are not available, blind adaptive algorithms, such as the constant modulus algorithm (CMA) [1], [53], can be developed to exploit a known property of the desired signal, for instance the constant-modulated signal envelope.

5. Direction of Arrival Estimation

Source DOA estimation is a principle function of sensor array processing, and the problem has received considerable attention in the literature [59]-[90]. In this section, we discuss four typical techniques: a) MVDR, also known as an optimal beamformer; b) MUSIC, one of the most well-known and studied schemes; c) ESPRIT, a computation efficient technique; and d) ML, a statistically optimal algorithm representing the best performance achievable. The discussion gives the reader a good foundation to understand other DOA estimators. The application of the algorithms for mobile communications has been investigated in [26]-[30], [32] and [88]-[90].

Consider the data model (18). In most DOA literature, the number of sources N is assumed to be known (given or estimated). The estimation of N is often referred to as the detection problem [54]-[55]. The Akaike's information criterion (AIC) [56] and minimum description length (MDL) [57] algorithms are among the most referred techniques. We also assume that the number of sensors is greater than the number of sources, $M > N$, to guarantee the uniqueness of DOA estimation [58].

5.a. MVDR Estimator

The MVDR beamformer can estimate the source DOA by computing the power spectrum (the mean output power of the array as a function of the direction) and then determining the local maxima. The result estimator is also known as the Capon's algorithm [41]. If we steer the array in direction θ, the weights can be obtained by minimizing the mean output power subject to unity constraint in the look direction as discussed in Section 4.c, and $\mathbf{w}(\theta) = \dfrac{\mathbf{R}^{-1}\mathbf{a}(\theta)}{\mathbf{a}^H(\theta)\mathbf{R}^{-1}\mathbf{a}(\theta)}$. An expression for the power spectrum is given by

$$P(\theta) = E\left\{\left|\mathbf{w}^H(\theta)\mathbf{y}(t)\right|^2\right\} = \left[\mathbf{a}^H(\theta)\mathbf{R}^{-1}\mathbf{a}(\theta)\right]^{-1}. \tag{44}$$

The DOA estimates are obtained by viewing the peaks in the spectrum. Similarly, the conventional beamformer can also be used for DOA estimation by computing the power spectrum

$$P(\theta) = E\left\{\left|\mathbf{w}^H(\theta)\mathbf{y}(t)\right|^2\right\} = \frac{\mathbf{a}^H(\theta)\mathbf{R}\,\mathbf{a}(\theta)}{M^2}, \tag{45}$$

where the weights $\mathbf{w}(\theta) = \frac{1}{M}\mathbf{a}(\theta)$ steer the array in direction θ. The resolving power of the conventional beamformer depends on the beamwidth of the main lobe, which is known as the conventional resolution limit. As expected, the MVDR estimator demonstrates better resolution properties than the conventional beamformer [59].

5.b. Multiple Signal Classification (MUSIC) Estimator

MUSIC [60] exploits the eigenstructure of the data covariance matrix (24), and can be classified as an eigenstructure method. The rationale for this class of algorithms is related to division of information in the data covariance matrix into two vector subspaces, namely, the signal subspace and the noise subspace. These algorithms assume that signals of interest lie in a lower dimensional signal space than the full dimensional space spanned by the data samples [61].

From (24), the data covariance matrix is given by $\mathbf{R} = \mathbf{A}\mathbf{P}\mathbf{A}^H + \sigma_n^2\mathbf{I}$. Assume the N sources to be uncorrelated, thus $\mathbf{P}$ is a diagonal matrix. Now, we can apply eigenvalue decomposition to $\mathbf{R}$. Under ideal conditions, the eigenvalues satisfy

$$\underbrace{\lambda_1 \geq \lambda_2 \geq \cdots \geq \lambda_N}_{N} > \underbrace{\sigma_n^2 = \cdots = \sigma_n^2}_{M-N}, \tag{46}$$

where λ_i $(i = 1, \cdots, N)$ are principal eigenvalues, all noise eigenvalues equal to σ_n^2, and the number of multiplicity is $M - N$. Assume that $\mathbf{q}_i$ $(i = 1, \cdots, M)$ are eigenvectors associated with ordered λ_i. $\mathbf{q}_i$ $(i = 1, \cdots, N)$ are principal eigenvectors, and $\mathbf{q}_i$ $(i = N+1, \cdots, M)$ are noise eigenvectors. The representation of $\mathbf{R}$ in terms of its eigenvalues and corresponding eigenvectors is as follows:

$$\mathbf{R} = \sum_{i=1}^{N}\left(\lambda_i - \sigma_n^2\right)\mathbf{q}_i\mathbf{q}_i^H + \sigma_n^2\mathbf{I}. \tag{47}$$

Since the signals are uncorrelated, $\mathbf{R}$ can also be expressed as

$$\mathbf{R} = \sum_{i=1}^{N} \left| p_i \right|^2 \mathbf{a}\left(\theta_i\right) \ \mathbf{a}^H\left(\theta_i\right) + \sigma_n^2 \mathbf{I}, \tag{48}$$

where $\left| p_i \right|^2$ is the average power of the *i*th source. Therefore,

$$\mathbf{APA}^H = \sum_{i=1}^{N} \left(\lambda_i - \sigma_n^2\right) \mathbf{q}_i \mathbf{q}_i^H = \sum_{i=1}^{N} \left| p_i \right|^2 \mathbf{a}\left(\theta_i\right) \mathbf{a}^H\left(\theta_i\right). \tag{49}$$

It means that the principal eigenvectors $\mathbf{q}_i$ ($i = 1, \cdots, N$) are linear combinations of array steering vectors $\mathbf{a}\left(\theta_i\right)$ associated with *N* sources, and vice versa. Equivalently, the vectors $\mathbf{q}_i$ ($i = 1, \cdots, N$) and $\mathbf{a}\left(\theta_i\right)$ span the same vector subspace – the signal subspace. And the noise eigenvectors $\mathbf{q}_i$ ($i = N+1, \cdots, M$) span the noise subspace, which is orthogonal to the signal subspace.

Once the signal and noise subspaces have been estimated, a search for *N* directions is made by looking for steering vectors that are as orthogonal to the noise subspace as possible. Let

$$\mathbf{U}_S = \left[\mathbf{q}_1 \quad \mathbf{q}_2 \quad \cdots \quad \mathbf{q}_N\right],$$

$$\mathbf{U}_N = \left[\mathbf{q}_{N+1} \quad \mathbf{q}_{N+2} \quad \cdots \quad \mathbf{q}_M\right], \tag{50}$$

the MUSIC algorithm can be written as [60]

$$P\left(\theta\right) = \frac{1}{\mathbf{a}^H\left(\theta\right) \mathbf{U}_N \mathbf{U}_N^H \mathbf{a}\left(\theta\right)}. \tag{51}$$

Instead of using the noise subspace, one may use the signal subspace and search for directions with steering vectors contained in this space. This amounts to searching for peaks in [62]

$$P\left(\theta\right) = \mathbf{a}^H\left(\theta\right) \mathbf{U}_S \mathbf{U}_S^H \mathbf{a}\left(\theta\right). \tag{52}$$

It is advantageous to use the one with smaller dimensions in (51) and (52). In practice, the estimates $\hat{\mathbf{U}}_S$ and $\hat{\mathbf{U}}_N$ are used, which are computed from the eigen-decomposition of the sample covariance matrix $\hat{\mathbf{R}}$ (25). The equations in (51) and (52) are the standard forms, known as spectral MUSIC. For ULAs, root-MUSIC [62], a polynomial rooting version of MUSIC, provides higher resolution capabilities. A weighted version of MUSIC, WMUSIC [63], also gives an extension in the resolution capabilities compared to spectral MUSIC.

5.c. Estimation of Signal Parameters via Rotational Invariance Technique (ESPRIT)

ESPRIT [64] is a computationally efficient eigenstructure method, which is free from searching peaks in pseudo spectrum as in previous methods. It requires that all sensors are present in pair-wise matched and co-directional doublets.

To describe mathematically the effect of the translation invariance of the sensor array, it is convenient to describe the array as being composed of two sub-arrays, identical in every aspect although physically displaced from each other by a known displacement vector $\mathbf{\Delta}$ of magnitude Δ measured in wavelengths. Following the data model (18), the outputs of two sub-arrays can be written as

$$\mathbf{x}(t) = \mathbf{A}\mathbf{s}(t) + \mathbf{n}_x(t),$$

$$\mathbf{y}(t) = \mathbf{A}\mathbf{\Phi}\mathbf{s}(t) + \mathbf{n}_y(t), \tag{53}$$

where $\mathbf{s}(t)$ is the vector of signals observed at the reference sensor of the sub-array corresponding to $\mathbf{x}(t)$, and $\mathbf{\Phi}$ is a diagonal matrix of phase delays between doublet sensors for *N* wavefronts, which is given by

$$\mathbf{\Phi} = diag\ \left\{ e^{j2\pi\Delta\cos\theta_1},\ \ldots,\ e^{j2\pi\Delta\cos\theta_N} \right\}, \tag{54}$$

and θ_i ($i = 1, \cdots, N$) is measured relative to the direction of $\mathbf{\Delta}$. The sub-array outputs can be combined to yield the total array output vector $\mathbf{z}(t)$ as

$$\mathbf{z}(t) = \begin{bmatrix} \mathbf{x}(t) \\ \mathbf{y}(t) \end{bmatrix} = \bar{\mathbf{A}}\,\mathbf{s}(t) + \mathbf{n}_z(t), \tag{55}$$

where

$$\bar{\mathbf{A}} = \begin{bmatrix} \mathbf{A} \\ \mathbf{A}\mathbf{\Phi} \end{bmatrix},\ \mathbf{n}_z(t) = \begin{bmatrix} \mathbf{n}_x(t) \\ \mathbf{n}_y(t) \end{bmatrix}.$$

Let $\mathbf{E}_X$ and $\mathbf{E}_Y$ be two sets of vectors, which span the signal subspace associated with $\mathbf{x}(t)$ and $\mathbf{y}(t)$ as in (50), respectively. If the output of sub-arrays is sampled simultaneously, $\mathbf{E}_X$ and $\mathbf{E}_Y$ span the same signal subspace. The basic idea behind ESPRIT is to exploit the rotational invariance of the underlying signal subspace.

The signal subspace can also be obtained from the covariance matrix $\mathbf{R}_z$ of $\mathbf{z}(t)$ as in (50), and denote it $\mathbf{E}_S$, where

$$\mathbf{R}_{\mathbf{z}} = E\left\{\mathbf{z}(t)\mathbf{z}^{H}(t)\right\} = \bar{\mathbf{A}}\mathbf{P}\bar{\mathbf{A}}^{H} + \sigma_n^2\mathbf{I}. \tag{56}$$

At the same time, the signal subspace can be spanned by the columns of $\bar{\mathbf{A}}$, namely $\Re\{\mathbf{E}_S\} = \Re\{\bar{\mathbf{A}}\}$. Therefore, there must exist a unique, nonsingular matrix $\mathbf{T}$ such that

$$\mathbf{E}_S = \bar{\mathbf{A}}\mathbf{T}. \tag{57}$$

Furthermore, the invariance structure of the array implies $\mathbf{E}_S$ can be decomposed into $\mathbf{E}_X$ and $\mathbf{E}_Y$ such that

$$\mathbf{E}_S = \begin{bmatrix}\mathbf{E}_X \\ \mathbf{E}_Y\end{bmatrix} = \begin{bmatrix}\mathbf{AT} \\ \mathbf{A\Phi T}\end{bmatrix}, \tag{58}$$

from which it is easily seen that

$$\Re\{\mathbf{E}_X\} = \Re\{\mathbf{E}_Y\} = \Re\{\mathbf{A}\}. \tag{59}$$

Therefore, there must exist a unique, nonsingular matrix $\mathbf{\Psi}$, such that $\mathbf{E}_X\mathbf{\Psi} = \mathbf{E}_Y$. Since $\mathbf{E}_X$ and $\mathbf{E}_Y$ share a common column space, the rank of $\mathbf{E}_{XY} = [\mathbf{E}_X \mid \mathbf{E}_Y]$ is *N*, which implies that there exists a unique rank *N* matrix $\mathbf{F}$ such that

$$\mathbf{0} = [\mathbf{E}_X \mid \mathbf{E}_Y]\mathbf{F} = \mathbf{E}_X\mathbf{F}_X + \mathbf{E}_Y\mathbf{F}_Y = \mathbf{ATF}_X + \mathbf{A\Phi TF}_Y, \tag{60}$$

where $\mathbf{F} = \begin{bmatrix}\mathbf{F}_X \\ \mathbf{F}_Y\end{bmatrix}$ spans the null-space of $[\mathbf{E}_X \mid \mathbf{E}_Y]$. Defining $\mathbf{\Psi} \overset{\text{def}}{=} -\mathbf{F}_X[\mathbf{F}_Y]^{-1}$, equation (60) can be rearranged to yield $\mathbf{AT\Psi T}^{-1} = \mathbf{A\Phi}$. Assuming $\mathbf{A}$ to be full rank implies

$$\mathbf{T\Psi T}^{-1} = \mathbf{\Phi}. \tag{61}$$

Therefore, eigenvalues of $\mathbf{\Psi}$ must be equal to diagonal elements of $\mathbf{\Phi}$, and DOA estimates can be obtained using

$$\theta_i = \cos^{-1}\left\{\frac{\arg(\lambda_i)}{2\pi\Delta}\right\}, \quad i = 1,\cdots,N, \tag{62}$$

where λ_i ($i = 1,\cdots,N$) are principal eigenvalues of $\mathbf{\Psi}$, and arg(·) denotes the phase angle. ESPRIT also has some important variations, including multiple invariance ESPRIT [65], virtual interpolated array ESPRIT [66], resolution-enhanced ESPRIT [67], and higher order ESPRIT [68].

5.d. Maximum Likelihood (ML) Estimator

The ML technique estimates source DOAs by maximizing the log-likelihood function, which signifies that signals from those directions are most likely to cause the occurrence of given samples. The ML method produces superior estimates compared to other methods, especially in unfavorable conditions involving low SNR, short data samples, highly correlated or coherent sources, and small array apertures, and thus is of practical interest. It can be used as a standard to compare the performance of other methods. Regarding the source signals, there are two types of models in current use: conditional model, which assumes the signals to be deterministic and unknown sequences; and unconditional model, which assumes the signals to be random. These two models lead to different ML methods, termed CML and UML respectively [69].

5.d.1. Conditional Maximum Likelihood (CML) Estimator

Assume the signals $\mathbf{s}(t)$ to be deterministic and unknown sequences, and the noise $\mathbf{n}(t)$ to be stationary zero-mean white Gaussian process, $E\{\mathbf{n}(t)\mathbf{n}^H(t)\} = \sigma_n^2\mathbf{I}$, therefore $\mathbf{y}(t) \sim G(\mathbf{As}(t), \sigma_n^2\mathbf{I})$, where $G(\cdot)$ denotes Gaussian distribution.

The likelihood function of the snapshots $\mathbf{y}(1), \ldots, \mathbf{y}(L)$ is given by

$$L(\mathbf{y}(1), \cdots, \mathbf{y}(L)) = \prod_{t=1}^{L} \frac{1}{\pi \det[\sigma_n^2\mathbf{I}]} \exp\left(-\frac{1}{\sigma_n^2} \left| \mathbf{y}(t) - \mathbf{As}(t) \right|^2 \right), \tag{63}$$

where, $\det[\bullet]$ stands for the determinant. Thus, the log-likelihood function is

$$\ln L = -L \ln \pi - ML \ln \sigma_n^2 - \frac{1}{\sigma_n^2} \sum_{t=1}^{L} \left| \mathbf{y}(t) - \mathbf{As}(t) \right|^2 . \tag{64}$$

In (64), σ_n^2, $\boldsymbol{\theta}$ (in $\mathbf{A}(\boldsymbol{\theta})$) and $\mathbf{s}(t)$ are unknown parameters.

Firstly, we fix $\boldsymbol{\theta}$ and $\mathbf{s}(t)$, and calculate the derivatives of (64) with respect to σ_n^2,

$$\frac{\partial \ln L}{\partial \sigma_n^2} = -\frac{ML}{\sigma_n^2} + \frac{1}{\sigma_n^4} \sum_{t=1}^{L} \left| \mathbf{y}(t) - \mathbf{As}(t) \right|^2 . \tag{65}$$

We then get,

$$\sigma_n^2 = \frac{1}{ML} \sum_{t=1}^{L} \left| \mathbf{y}(t) - \mathbf{As}(t) \right|^2 . \tag{66}$$

Secondly, fixing σ_n^2 and $\boldsymbol{\theta}$, we calculate the derivatives of (64) with respect to $\mathbf{s}(t)$,

$$\frac{\partial \ln L}{\partial \mathbf{s}(t)} = \frac{2}{\sigma_n^2}\mathbf{A}^H\left[\mathbf{y}(t) - \mathbf{A}\mathbf{s}(t)\right], \tag{67}$$

it arrives at

$$\mathbf{s}(t) = \left(\mathbf{A}^H\mathbf{A}\right)^{-1}\mathbf{A}^H\mathbf{y}(t). \tag{68}$$

Finally, substituting (66) and (68) back into (64), we obtain the following maximization problem,

$$\arg\max_{\boldsymbol{\theta}}\left\{-ML\ln\frac{1}{ML}\sum_{t=1}^{L}\left|\mathbf{y}(t) - \mathbf{A}\left(\mathbf{A}^H\mathbf{A}\right)^{-1}\mathbf{A}^H\mathbf{y}(t)\right|^2\right\}, \tag{69}$$

which is equivalent to the following minimization problem

$$f_{CML}(\boldsymbol{\theta}) = \arg\min_{\boldsymbol{\theta}}\left\{tr\left[(\mathbf{I} - \mathbf{A}\left(\mathbf{A}^H\mathbf{A}\right)^{-1}\mathbf{A}^H)\hat{\mathbf{R}}\right]\right\}, \tag{70}$$

where $tr[\bullet]$ denotes the trace, and $\hat{\mathbf{R}}$ is the sample covariance matrix (25).

5.d.2. Unconditional Maximum Likelihood (UML) Estimator

If we assume that both the signals and the noise are stationary, temporally white, zero-mean complex Gaussian random processes with second-order moments satisfying (23), following a similar derivation procedure, we can conclude that the UML estimator is given by minimizing (71)

$$f_{UML}(\boldsymbol{\theta}) = \ln\det\left[\mathbf{A}\tilde{\mathbf{P}}\mathbf{A}^H + \tilde{q}\mathbf{I}\right], \tag{71}$$

where

$$\tilde{\mathbf{P}} = \left(\mathbf{A}^H\mathbf{A}\right)^{-1}\mathbf{A}^H\hat{\mathbf{R}}\mathbf{A}\left(\mathbf{A}^H\mathbf{A}\right)^{-1} - \tilde{q}\left(\mathbf{A}^H\mathbf{A}\right)^{-1},$$

$$\tilde{q} = \frac{1}{M-N}tr\left\{\left[\mathbf{I} - \mathbf{A}\left(\mathbf{A}^H\mathbf{A}\right)^{-1}\mathbf{A}^H\right]\hat{\mathbf{R}}\right\},$$

and $\ln[\bullet]$ denotes the natural logarithm.

Literature [69] demonstrates that for uncorrelated sources, the statistical performances of CML and UML are similar; while for highly correlated or coherent sources, UML is significantly superior. For UML, the stochastic Cramer-Rao bound (CRB) can be achieved as $N \to \infty$ or $\text{SNR} \to \infty$; while for CML, the corresponding bound cannot be attained if $M < \infty$, even though $N \to \infty$ or $\text{SNR} \to \infty$.

The optimization of likelihood functions (70) and (71) is a nonlinear optimization problem. In the absence of a closed form solution, it requires iterative schemes for

solutions. Many such schemes have been proposed for solving this problem, such as the alternating projection method [70], the simulated annealing method [71], the expectation maximization algorithm [72], and the data supported grid search technique [73]. A fast algorithm [74]-[76] based on a modified genetic algorithm is presented for solutions in general cases.

5.e. Performance Evaluation and Comparison

The main performance measures for a DOA estimator include bias, variance, and probability of resolution, which are complicated functions of source SNR, data sample size, number and directions of sources, and array geometry. A poor estimate generally results from using shorter snapshots and sources with lower SNR. Even though bias and variance both play important roles in direction estimation, the effect of bias is more critical in the threshold region. The variance is often evaluated against the CRB, which provides a lower bound on the covariance matrix of any unbiased estimator and is expected to be a good performance predictor for large samples.

The stochastic CRB associated with DOA estimation in white Gaussian noise is given by [77]

$$\mathrm{CRB}(\boldsymbol{\theta}) = \frac{\sigma_n^2}{2L}\left[\mathrm{Re}\left\{ \left[\mathbf{D}^H \mathbf{P}_A^{\perp} \mathbf{D} \right] \odot \left[\mathbf{P}\mathbf{A}^H \mathbf{R}^{-1} \mathbf{A}\mathbf{P} \right]^T \right\} \right]^{-1}, \tag{72}$$

where $\mathbf{X} \odot \mathbf{Y}$ denotes the Hadamard product of matrices **X** and **Y**, i.e., $(\mathbf{X} \odot \mathbf{Y})_{ij} = \mathbf{X}_{ij}\mathbf{Y}_{ij}$, **P** is the signal covariance matrix, and

$$\mathbf{P}_A^{\perp} = \mathbf{I} - \mathbf{A}\left(\mathbf{A}^H \mathbf{A} \right)^{-1} \mathbf{A}^H,$$

$$\mathbf{D} = \left[\left. \frac{\partial \mathbf{a}(\theta)}{\partial \theta} \right|_{\theta=\theta_1} \cdots \left. \frac{\partial \mathbf{a}(\theta)}{\partial \theta} \right|_{\theta=\theta_N} \right]. \tag{73}$$

In the follows, we present a numerical example to compare the performance of UML, ESPRIT, MUSIC and MVDR, and evaluate those estimators against the CRB. Each simulated point is calculated based on 500 independent Monte-Carlo trials. The performances of those methods are compared at two aspects: a) DOA estimation root-mean-squared error (RMSE), which is calculated as

$$RMSE = \sqrt{\frac{1}{NN_{runs}} \sum_{l=1}^{N_{runs}} \sum_{i=1}^{N} [\hat{\theta}_i(l) - \theta_i]^2}, \tag{74}$$

where N is the number of sources, $\hat{\theta}_i(l)$ is the estimate of the ith DOA achieved in the lth run, θ_i is the true DOA of the ith source; b) the ability to resolve closely spaced sources.

By definition, two sources are said to be resolved in a given run if $\left|\hat{\theta}_i - \theta_i\right| < \left|\theta_1 - \theta_2\right|/2$, $i = 1, 2$ are satisfied.

Since ESPRIT requires two displaced subarrays of matched doublets and is only applicable to certain geometry such as ULA, an 8-element ULA with half-wavelength element spacing is considered. Because correlated sources due to, for example multipath propagation are of practical interest in mobile communications, two equal-power correlated signals with the correlation factor $\gamma = 0.8$ are assumed to illuminate the array from 61° and 64° relative to the end-fire. The number of snapshots is 40, and SNR is varied.

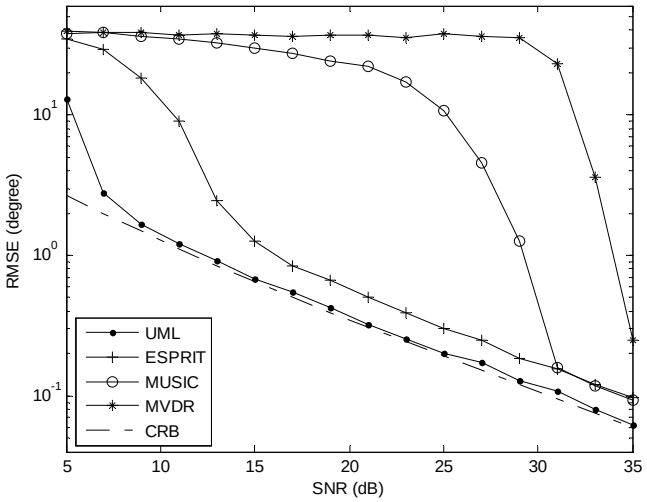

Figure 7. DOA estimation RMSE of UML, ESPRIT, MUSIC and MVDR versus SNR.

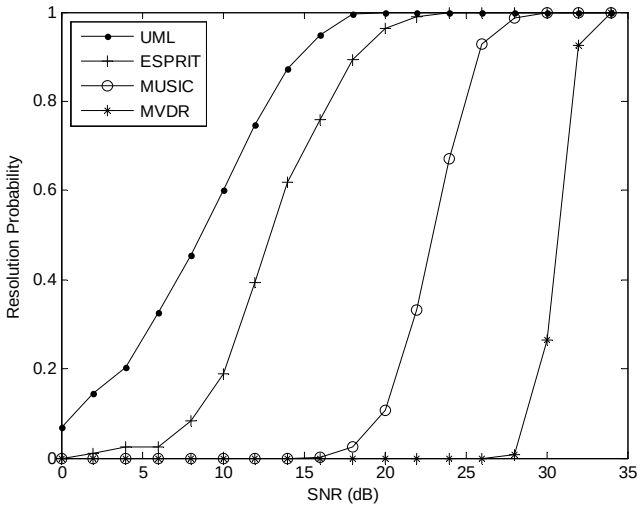

Figure 8. Resolution probabilities of UML, ESPRIT, MUSIC and MVDR versus SNR.

Figure 7 depicts DOA estimation RMSE obtained by UML, ESPRIT, MUSIC and MVDR, and compares them with the CRB. Figure 8 shows the resolution probabilities for the same methods. As can be seen from Figure 7 – Figure 8, UML demonstrates much better performance than the other techniques as a whole, producing more accurate estimates in terms of RMSE, and better source resolving power in terms of resolution probabilities. UML asymptotically attains the CRB when SNR gets higher. ESPRIT performs better than MUSIC and MVDR in the cases of correlated sources, and MVDR demonstrates the strongest threshold effect when SNR is small. Based on the simulation results and performance analysis carried out in the literature, we make some comments on pros and cons of each algorithm for performance evaluation.

1. UML is statistically optimal and yields superior estimates. It can tackle correlated or even coherent arrivals. For Gaussian signals, the estimates of UML are unbiased and efficient. However, UML is computation intensive due to optimization of the multi-dimensional multimodal likelihood function. [69], [77]-[78].
2. MUSIC estimates are the large sample realization of ML estimates in the presence of uncorrelated arrivals, and asymptotically efficient for large arrays. A rigorous bias analysis shows that MUSIC estimates are biased. MUSIC makes a good compromise between computation and accuracy, and is one of the most studied schemes. [77], [79]-[81].
3. ESPRIT is computation-efficient with advantages over other algorithms such as speed, storage, and indifference to array calibration. ESPRIT and MUSIC are two important eigenstructure methods: ESPRIT may yield unbiased estimates with variance less than MUSIC; ESPRIT is more robust than MUSIC and can handle correlated arrivals; but ESPRIT requires specific array geometry. [64], [80], [82]-[83].
4. MVDR is suitable for both DOA estimation and optimal beamforming, which is less sensitive to perturbations and model errors than ML, MUSIC and ESPRIT. [59], [84]-[85].

6. Conclusion

Smart antennas are often classified as either switched-beam or adaptive-array systems. Each class of smart antennas has its own inherent cost-complexity trade off. The relative merits of both implementations for ITS have been discussed. This chapter deals with the signal processing aspects of smart antenna systems. In general, smart antenna system design and algorithm selection are a trade-off between complexity and performance. Various beamforming algorithms using spatial and temporal reference, and the adaptive implementations are described. DOA estimation is an essential function of antenna arrays, which can be utilized to orient the beamformer or be exploited for location positioning. There exists many DOA estimation algorithms with conflicting demands of accuracy and computation. Some of the typical algorithms are discussed and analyzed.

Smart antennas technology will have significant impact on future intelligent transportation systems. It will support various transportation applications, trigger many new services, and make the future ITS to be less complex while providing more attractive and convenient services. It is believed that this technology has great potential to make transportation systems operate more safely and efficiently, with less congestion, pollution, and environmental impact.

References

[1] Liberti, J. and Rappaport, T. *Smart Antennas for Wireless Communications: IS-95 and Third Generation CDMA Applications.* Upper Saddle River, NJ: Prentice-Hall, 1999.

[2] Drane, C. and Rizons, C. *Positioning Systems in Intelligent Transportation Systems.* Norwood, MA: Artech House, 1998.

[3] Chryssomallis, M. Smart antennas. *IEEE Antennas and Propagation Magazine.* 2000;42:129-136.

[4] Zhao, Y. Mobile phone location determination and its impact on intelligent transportation systems. *IEEE Transactions on Intelligent Transportation Systems.* 2000;1:55-64.

[5] Zhao, Y. *Vehicle Location and Navigation Systems.* Norwood, MA: Artech House, 1997.

[6] Bellofiore, S., Balanis, C., Foutz, J. and Spanias, A. Smart-antenna systems for mobile communication networks. Part 1. Overview and antenna design. *IEEE Antennas and Propagation Magazine*, 2002;44:145-154.

[7] Bellofiore, S., Foutz, J., Balanis, C. and Spanias, A. Smart-antenna system for mobile communication networks. Part 2. Beamforming and network throughput. *IEEE Antennas and Propagation Magazine.* 2002;44:106-114.

[8] Li B, Wang H, Yan B, Zhang C. The research of applying wireless sensor networks to intelligent transportation system (ITS) based on IEEE 802.15.4. in *Proceedings of 6th International Conference on ITS Telecommunications*. 2006; 939-942.

[9] Chen W, Chen L, Chen Z, Tu S. WITS: A wireless sensor network for intelligent transportation system. in *Proceedings of First International Multi-Symposiums on Computer and Computational Sciences*. 2006; 2: 635-641.

[10] Sawant H, Tan J, Yang Q. A sensor networked approach for intelligent transportation systems. in *Proceedings IEEE/RSJ International Conference on Intelligent Robots and Systems (IROS 2004)*. 2004; 2:1796-1801.

[11] Giorgetti G, Cidronali A, Gupta S, Manes G. Exploiting low-cost directional antennas in 2.4 GHz IEEE 802.15.4 wireless sensor networks. in *Proceedings 10th European Conference on Wireless Technologies*. 2007; 217-220.

[12] Bellofiore, S., Foutz, J., Govindarajula, R., Bahceci, I., Balanis, C., Spanias, A, Capone, J. and Duman, T. Smart antenna system analysis, integration, and performance for mobile ad-hoc networks (MANETs). *IEEE Transactions on Antennas and Propagation*. 2002;50: 571-581.

[13] Koubaa, H. Reflections on smart antennas for MAC protocols in multihop ad hoc networks. in *Proceedings European Wireless'02*. 2002; 25-28.

[14] Singh, H. and Singh, S. Tone based MAC protocol for use with adaptive array

antennas. in *Proceedings IEEE WCNC 2004*. 2004; 1246-1251.
[15] Johnson, D., Dudgeon, D. *Array signal processing*. USA, Prentice-Hall, 1993.
[16] Tsoulos, G., Approximate SIR and BER formulas for DS-CDMA based on radiation pattern characteristics of adaptive antennas. *Electronics Letters*. 1998;34:1802-1804.
[17] Hata, M. Empirical formula for propagation loss in land mobile radio services. *IEEE Transactions on Vehicular Technology*. 1980;29:317-325.
[18] Yacoub, M. *Foundations of Mobile Radio Engineering*. CRC Press, 1993.
[19] Dakdouki, A., Banket, V., Mykhaylov, N. and Skopa, A. Downlink processing algorithms for multi-antenna wireless communications. *IEEE Communications Magazine*. 2005;43: 122-127.
[20] Winters, J., Salz, J. and Gitlin, R. The impact of antenna diversity on the capacity of wireless communications systems. *IEEE Transactions on Communications*. 1994;42:1740-1751.
[21] Klukas, R., Lachapelle, G. and Fattouche M. Field tests of a cellular telephone positioning system. in *Proceedings 47th IEEE Vehicular Technologies Conference*. 1997;2:470-474.
[22] Rappaport, T., Reed, J. and Woerner, B. Position location using wireless communications on highways of the future. *IEEE Communications Magazine*. 1996;34:33-41.
[23] O'Connor, J., Alexander, B. and Schorman, E. CDMA infrastructure-based location finding for E911. in *Proceedings 49th IEEE Vehicular Technology Conference*. 1999;3:1973-1978.
[24] Gutowski, G., Jalloul, L., Golovin, E., Nakhjiri, M., Yousef, N. and DeClerck, P. Simulation results of CDMA location finding systems. in *Proceedings 49th IEEE Vehicular Technology Conference*. 1999;3:2124-2128.
[25] Niculescu, D. and Nath, B. Ad hoc positioning system (APS) using AOA. in *Proceedings IEEE INFOCOM 2003*, 2003; 1734-1743.
[26] Xiong, L. A selective model to suppress NLOS signals in angle-of-arrival (AOA) location estimation. in *Proceedings 9th IEEE International Symposium Personal, Indoor and Mobile Radio Communications (PIMRC'98)*. 1998;1:461-465.
[27] Owen, R. and Lopes, L. Experimental analysis of the use of angle of arrival at an adaptive antenna array for location estimation. in *Proceedings 9th IEEE International Symposium Personal, Indoor and Mobile Radio Communications (PIMRC'98)*, 1998;2:607-611.
[28] Qi, Y., Kobayashi, H. and Suda, H. Analysis of wireless geolocation in a non-line-of-sight environment. *IEEE Transactions on Wireless Communications*. 2006;5:672-681.
[29] Gu, Z. and Gunawan, E. Radiolocation in CDMA cellular system based on joint angle and delay estimation. *Wireless Personal Communications*. 2002;23:297-309.
[30] Cong, L. and Zhuang, W. Hybrid TDOA/AOA mobile user location for wideband CDMA cellular systems. *IEEE Transactions on Wireless Communications*. 2002;1:439-447.
[31] Kleine-Ostmann, T. and Bell, A. A data fusion architecture for enhanced position estimation in wireless networks. *IEEE Communications Letters*. 2001;5:343-345.
[32] Litva, J and Lo, T. *Digital Beamforming in Wireless Communications*. Artech, 1996.
[33] Bartlett, M. *An Introduction to Stochastic Process*. New York: Cambridge

University Press, 1956.
[34] Johnson, D. The application of spectral estimation methods to bearing estimation problems. *Proceedings IEEE*. 1982;70:1018-1028.
[35] Anderson, V. DICANNE, a realizable adaptive process. *Journal of the Acoustical Society of America*. 1969;45:398-405.
[36] Friedlander, B. and Porat, B. Performance analysis of a null-steering algorithm based on direction-of-arrival estimation. *IEEE Transactions on Acoustics, Speech, and Signal Processing*. 1989;37:461-466.
[37] Murino, V., Trucco, A. and Regazzoni, C. Synthesis of equally spaced arrays by simulated annealing. *IEEE Transactions on Signal Processing*. 1996;44:119-122.
[38] Yan, K. K. and Lu, Y. L. Sidelobe reduction in array-pattern synthesis using genetic algorithm. *IEEE Transactions on Antennas and Propagation*. 1997;45:1117-1122.
[39] Khodier, M. and Christodoulou, C. Linear array geometry synthesis with minimum sidelobe level and null control using particle swarm optimization. *IEEE Transactions on Antennas and Propagation*. 2005;53:2674-2679.
[40] Li, M. H. and Lu, Y. L. Dimension reduction for array processing with robust interference cancellation. *IEEE Transactions on Aerospace and Electronic Systems*. 2006;42:103-112.
[41] Capon, J. High-resolution frequency-wave number spectrum analysis. *Proceedings IEEE*. 1969;57:1408-1418.
[42] Winters, J. Optimum combining in digital mobile radio with cochannel interference. *IEEE Journal on Selected Areas in Communications*. 1984;2:528-539.
[43] Winters, J. Optimum combining for indoor radio systems with multiple users. *IEEE Transactions on Communications*. 1987;35:1222-1230.
[44] Suard, B., Naguib, A., Xu, G. and Paulraj, A. Performance of CDMA mobile communication systems using antenna arrays. in *Proceedings ICASSP-93*. 1993; 153-156.
[45] Griffiths, L. A comparison of multidimensional Weiner and maximum-likelihood filters for antenna arrays. *Proceedings IEEE*. 1967;55:2045-2047.
[46] Anderson, S., Millnert, M., Viberg, M. and Wahlberg, B. An adaptive array for mobile communication systems. *Transactions on Vehicular Technology*. 1991;40:230-236.
[47] Gebauer, T., Gockler, H. Channel-individual adaptive beamforming for mobile satellite communications. *IEEE Journal on Selected Areas in Communications*. 1995;13:439-448.
[48] Lindskog, E. Making SMI-beamforming insensitive to the sampling timing for GSM signals. in *Proceedings 6th IEEE International Symposium Personal, Indoor and Mobile Radio Communications (PIMRC'95)*. 1995;2:664-668.
[49] Passerini, C., Missiroli, M., Riva, G. and Frullone, M. Adaptive antenna arrays for reducing the delay spread in indoor radio channels. *Electronics Letters*. 1996;32:280-281.
[50] Widrow, B., Mantey, P., Griffiths, L. and Goode, B. Adaptive antenna systems. *Proceedings IEEE*. 1967;55:2143-2158.
[51] Haykin, S. *Adaptive Filter Theory*. Prentice Hall, 3rd ed., 1995.
[52] Jones, M. and Wickert, M. Direct sequence spread spectrum using directionally constrained adaptive beamforming to null interference. *IEEE Journal on Selected Areas in Communications*. 1995;13:71-79.
[53] Treichler, J. and Agee, B. A new approach to multipath correction of constant

modulus signals. *IEEE Transactions on Acoustics, Speech, and Signal Processing*. 1983;31:459-472.
[54] Wax, M. and Kailath, T. Detection of signals by information theoretic criteria. *IEEE Transactions on Acoustics, Speech, and Signal Processing*. 1985;33:387-392.
[55] Fuchs, J. Estimating the number of sinusoids in additive white noise. *IEEE Transactions on Acoustics, Speech, and Signal Processing*. 1988;36:1846-1854.
[56] Akaike, H. A new look at the statistical model identification. *IEEE Transactions on Automatic Control*. 1974;19:716-723.
[57] Rissanen, J. Modeling by shortest data description. *Automatica*. 1978;14:465-471.
[58] Wax, M. and Ziskind, I. On unique localization of multiple sources by passive sensor arrays. *IEEE Transactions on Acoustics, Speech, and Signal Processing*. 1989;37:996-1000.
[59] Cox, H. Resolving power and sensitivity to mismatch of optimum array processors. *Journal of the Acoustical Society of America*. 1973;54:771-785.
[60] Schmidt, R. Multiple emitter location and signal parameter estimation, *IEEE Transactions on Antennas and Propagation*. 1986;34:276-280.
[61] Tufts, D. and Melissinos, C. Simple, effective computation of principal eigenvectors and their eigenvalues and application to high-resolution estimation of frequencies. *IEEE Transactions on Acoustics, Speech, and Signal Processing*. 1986;34:1046-1053.
[62] Barabell, A. Improving the resolution of eigenstructure based direction finding algorithm. in *Proceedings ICASSP-83*. 1983; 336-339.
[63] Kaveh, M. and Bassias, A. Threshold extension based on a new paradigm for MUSIC-type estimation. in *Proceedings ICASSP-90*. 1990;5:2535-2538.
[64] Roy, R. and Kailath, T. ESPRIT – Estimation of signal parameters via rotational invariance techniques. *IEEE Transactions on Acoustics, Speech, and Signal Processing*. 1989;37: 984-995.
[65] Swindlehurst, A., Ottersten, B., Roy, R. and Kailath, T. Multiple invariance ESPRIT. *IEEE Transactions on Signal Processing*. 1992;40:867-881.
[66] Gavish, M. and Weiss, A. Performance analysis of the VIA-ESPRIT algorithm. *IEE Proceedings -F*, 1993;140:123-128.
[67] Hamza R, Buckley K. Resolution enhanced ESPRIT. *IEEE Transactions on Signal Processing*. 1994;42:688-691.
[68] Yuen N, Friedlander B. Asymptotic performance analysis of ESPRIT, higher order ESPRIT, and virtual ESPRIT algorithms. *IEEE Transactions on Signal Processing*. 1996;44:2537-2550.
[69] Stoica, P. and Nehorai, A. Performance study of conditional and unconditional direction-of-arrival estimation. *IEEE Transactions on Acoustics, Speech, and Signal Processing*. 1990;38:1783-1795.
[70] Ziskind, I. and Wax, M. Maximum likelihood localization of multiple sources by alternating projection. *IEEE Transactions on Acoustics, Speech, and Signal Processing*. 1988;36: 1553-1560.
[71] Sharman K. Maximum likelihood estimation by simulated annealing. in *Proceedings ICASSP-88*. 1988; 2741-2744.
[72] Miller M, Fuhrmann D. Maximum likelihood narrow-band direction finding and the EM algorithm. *IEEE Transactions on Acoustics, Speech, and Signal Processing*. 1990; 38:1560-1577.
[73] Stoica, P. and Gershman, A. Maximum-likelihood DOA estimation by data-

supported grid search. *IEEE Signal Processing Letters*. 1999;6:273-275.
[74] Li, M. H. and Lu, Y. L. Genetic algorithm based maximum likelihood DOA estimation. in *Proceedings Radar 2002*. 2002; 502-506.
[75] Li, M. H. and Lu, Y. L. Improving the performance of GA-ML DOA estimator with a resampling scheme. *Signal Processing*. 2004;84:1813-1822.
[76] Li, M. H. and Lu, Y. L. Accurate direction-of-arrival estimation of multiple sources using a genetic approach. *Wireless Communications and Mobile Computing*. 2005;5:343-353.
[77] Stoica, P. and Nehorai, A. MUSIC, maximum likelihood, and Cramer-Rao bound. *IEEE Transactions on Acoustics, Speech, and Signal Processing*. 1989;37:720-741.
[78] Viberg, M., Ottersten, B. and Nehorai, A. Performance analysis of direction finding with large arrays and finite data. *IEEE Transactions on Signal Processing*. 1995;43:469-477.
[79] Xu, X. and Buckley, K. Bias analysis of the MUSIC location estimator. *IEEE Transactions on Signal Processing*. 1992;40:2559-2569.
[80] Stoica, P. and Nehorai, A. Performance comparison of subspace rotation and MUSIC methods of direction estimation. *IEEE Transactions on Signal Processing*. 1991;39:446-453.
[81] Weiss, A. and Friedlander, B. Effect of modeling errors on the resolution threshold of the MUSIC algorithm. *IEEE Transactions on Signal Processing*. 1994;42:1519-1526.
[82] Ottersten, B., Viberg, M. and Kailath, T. Performance analysis of the total least squares ESPRIT algorithm. *IEEE Transactions on Signal Processing*. 1991;39:1122-1135.
[83] Soon, V. and Huans, Y. An analysis of ESPRIT under random sensor uncertainties. *IEEE Transactions on Signal Processing*. 1992;40:2353-2358.
[84] Lacoss, R. Data adaptive spectral analysis method. *Geophysics*. 1971;36:661-675.
[85] Nuttall, A., Carter, G. and Montaron, E. Estimation of two-dimensional spectrum of the space-time noise field for a sparse line array. *Journal of the Acoustical Society of America*. 1974;55:1034-1041.
[86] Li, M. H. and Lu, Y. L. Maximum likelihood DOA estimation in unknown colored noise fields. *IEEE Transactions on Aerospace and Electronic Systems*. 2008;44:1079-1090.
[87] Li, M. H. and Lu, Y. L. Source bearing and steering-vector estimation using partially calibrated arrays. *IEEE Transactions on Aerospace and Electronic Systems*. 2009;45.
[88] Biedka, T., Reed, J. and Woerner, B. Direction finding methods for CDMA systems. in *Proceedings 13th Asilomar Conference on Signals, Systems and Computers*. 1996;637-641.
[89] Wigren, T. and Eriksson, A. Accuracy aspects of DOA and angular velocity estimation in sensor array processing. IEEE Signal Processing Letters. 1995;2:60-62.
[90] Kluka, R. and Fattouche, M. Line-of-sight angle of arrival estimation in the outdoor multipath environment. *IEEE Transactions on Vehicular Technology*. 1998;47:342-351.